A 10 GHz Integrated Class-E Oscillating Annular Ring Element for High-Efficiency Transmitting Arrays

Joseph A. Hagerty and Zoya Popović

Joseph.Hagerty@Colorado.EDU
Department of Electrical and Computer Engineering,
University of Colorado
Boulder, CO 80309-0425 USA

Abstract— **An X-band oscillating element can be achieved in compact form with class-E operation and high directivity. An annular ring is used both as the radiating element and microstrip feedback circuit for the class-E amplifier. A maximum conversion efficiency of the dc power consumption to radiated co-polarized power is 55% at 10 GHz with maximum effective radiated power of 23.6 dBm and total radiated power of 15.5 dBm. This active antenna element is shown to be a good candidate for high aperture efficiency spatial power combining.**

I. Introduction

Free-space power combining of distributed oscillating elements presents a high-efficiency solution to microwave dc-rf conversion. By distributing sources in an array, transmission lines, combiners, and associated losses can be eliminated. Furthermore, the circuit size of the individual oscillating elements can be greatly reduced by incorporating the antenna element directly as a resonator and feedback circuit. Early designs have combined the radiating element as a load with a stand-alone oscillator and separate feedback loop. More recent designs have used rectangular patches as a radiator in the feedback path [1], [2], [3]. FETs were also directly integrated into the radiating element using modified antenna geometries for direct matching [4], [5]. Similarly a 100-MESFET grid oscillator capable of high output power and gain was first reported in [6].

Here, we investigate the additional advantages of using a compact single layer, high gain, switched mode integrated oscillating antenna. The performance of the unit cell is assessed as an element for a high- efficiency power combining array. A microstrip annular ring has been chosen to improve the radiation characteristics and reduce microstrip circuitry over conventional designs. The entire circuit is conveniently enclosed inside the ring allowing for straight-forward, compact array design. High-efficiency is afforded by switched mode transistor operation, high antenna gain, and high array packing density.

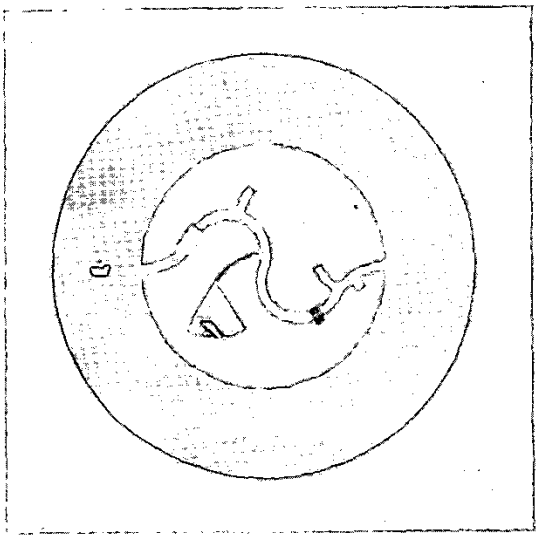

Fig. 1. Photograph of the microstrip annular ring with MESFET (dark-colored chip) and class-E circuit. The input impedance of the antenna feed to the right of the device is transformed to the class-E output load. The input matching circuit to the left of the device controls the degree of feedback. The outer diameter of the ring is 0.72 λ_0 at 10 GHz (21.6 mm).

II. Class-E Oscillation

Class-E amplifiers operate in switched mode: At the output, wave shaping is performed at the fundamental and second harmonic forcing the transistor to operate as a switch, while the current delivered to the load is sinusoidal. Under this mode of amplification, conductive losses in the transistor are theoretically eliminated and 100% drain efficiency is ideally attainable. Transmission-line microwave class-E am-

0-7803-7239-5/02/$10.00 © 2002 IEEE

plifiers have been demonstrated first in [7]. Recently drain efficiencies of 70% have been achieved at 10 GHz in [8] using the same Alpha MESFET as in the work reported here. A class-E oscillator with 59 % efficiency at 5 GHz has also been demonstrated in [9]. This oscillator was designed with an asymmetric branch-line coupler to provide -5.5 dB feedback.

In this paper, the techniques used for class-E matching and feedback for oscillation are modified for integration with a 2-port antenna. The calculated class-E load impedance at 10 GHz for the Alpha AFM04P2 transistor used here is $Z_E = 27.3 + j31.5\,\Omega$. This impedance is presented to the output of the transistor by transforming the antenna impedance using a second-harmonic termination and tuning stub. The antenna is designed as a 2-port structure with tunable coupling so that an additional coupler is not needed.

III. Antenna Design

The geometry of the annular ring was designed for radiative and selective feedback properties simultaneously. By virtue of the ring's cylindrical symmetry and thin height, the patch predominately supports circumferential and radial transverse magnetic field variations, denoted n and m. For the TM_{n1} modes, the field varies only along the circumference and subsequent resonances are narrow band compared to higher order modes. Theoretical field analysis was performed using Zeland *IE3D* MoM solver for current distributions on the patch and radiation patterns. Additional radiation behavior and modal analysis were studied using expressions derived from the cavity model of the ring [10], [11]. Here, the TM_{12} mode is used for several reasons. Despite its considerably higher operating frequency compared to the fundamental TM_{11} mode, the TM_{12} mode is used for its wider bandwidth. In our case, the wider bandwidth allows for higher tolerances in design and fabrication errors while maintaining a stable oscillation. The $m = 2$ variations along the circumference lead to a symmetric current distribution on two sides of the ring, offering two convenient feed points on the order of a half-wavelength apart. Furthermore, the ratio of the outer to inner radii, b/a, can be designed to improve radiation characteristics such as side-lobe level and lateral radiation as shown in Fig. 2. In effect, radiation from opposing sides of the ring can be designed to cancel lateral radiation in the E-plane, boosting the antenna gain and decreasing the coupling between arrayed elements [12].

Since several TM_{n1} modes occur at lower frequencies than the TM_{12} mode, care must be taken to ensure

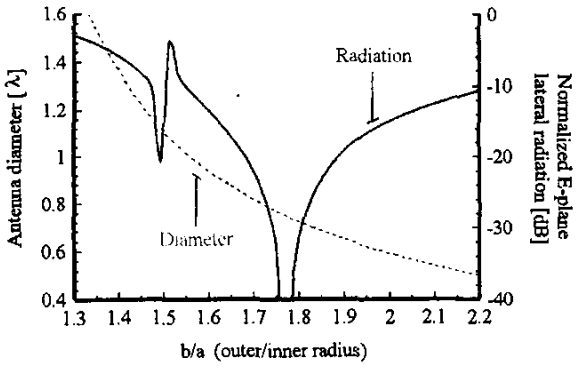

Fig. 2. Lateral radiated power normalized to broadside and antenna diameter as a function of b/a ratio for a 10 GHz ring on a TMM10i substrate with ϵ_r=9.8.

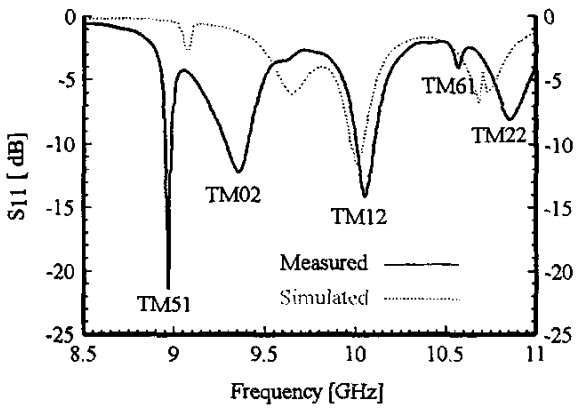

Fig. 3. Measured return loss of the passive microstrip annular ring. The TM_{12} mode is deigned to resonate at 10 GHz with b/a=1.75 (b=10.8 mm, a=6.17 mm).

that none of these modes meet an oscillation condition or overlap with the desired TM_{12} mode. The choice of b/a ratio can also be chosen to design unwanted modes out of the desired operation. Fig. 3 demonstrates the measured and simulated return loss and mode occurrence of the ring in a 50 Ω system.

IV. Integrated Class-E Annular Ring

The annular ring and class-E circuit with matching sections are designed separately and then analyzed as a complete circuit. Considering ports 1 and 2 of the ring as shown in Fig. 4, the input impedance, Z_{11}, of the antenna must be transformed to the class-E match, while S_{21} quantifies the feedback coupling factor. The magnitude of feedback coupling can be determined by the load presented to port-2 of the antenna. In this case, a load

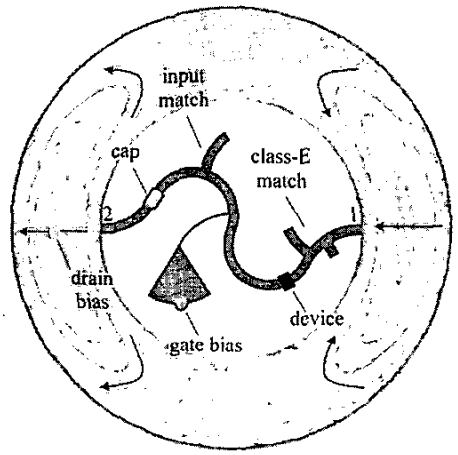

Fig. 4. Layout of the integrated ring with simulated average current amplitude distribution. Arrows indicate current density field lines.

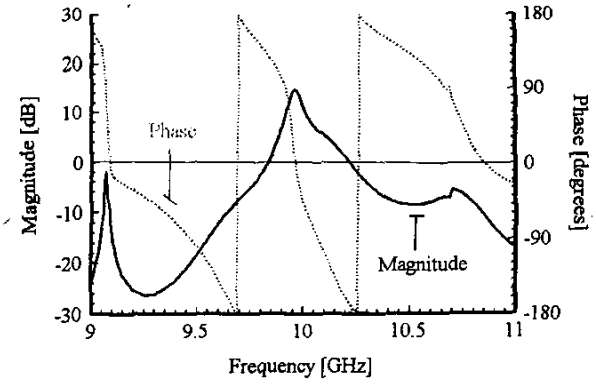

Fig. 5. Simulated closed loop gain of the oscillator.

of 280 Ω was chosen for -6.4 dB (23%) feedback. A line length is added to the input matching circuit to complete the $2\pi n$ closed loop phase. As expected from the simulated current distribution on the ring, the phase of S_{21} across the antenna is calculated to be just under π, while the transistor S_{21} phase is a little less than $\pi/2$. Therefore, the microstrip circuitry must add over $\pi/2$ in phase. forcing it to meander inside the ring.

Full-wave field analysis combined with measurements on a single-port passive ring are used to calculate the 2-port antenna parameters. Manufacturer specified 2-port transistor s-parameters were used in Agilent ADS to design the microstrip circuit. The calculated closed loop gain, shown in a magnitude/phase plot in Fig. 5, demonstrates that oscillations in adjacent antenna modes are eliminated.

V. Measurements

All measurements on the active ring were performed in a 4 m anechoic chamber. Broadside radiated power, oscillation frequency, and drain current were recorded over 644 bias points (from $V_{gs} = -0.6\,V$ and $V_{ds} = 0.6\,V$ to $V_{gs} = -2\,V$ and $V_{ds} = 5\,V$) using a computerized bias sweep of the gate and drain. The total radiated power and efficiency are calculated relative to a passive ring. The frequency of oscillation across the entire bias sweep varies by 1.5% of the design frequency. The measured ERP and DC power consumption for $V_{gs} = -1.3\,V$ are shown in Fig. 6 as a function of drain bias.

Measured radiation patterns at various bias points do not vary considerably as expected from the antenna bandwidth shown in Fig. 3. Figs. 7 and 8 show a comparison between the measured passive and active E and H-planes. The cross-polarized power at bore-sight is -28 dB. The laterally radiated power at 90° agrees well with the predicted values of Fig. 2 for a value of $b/a = 1.75$. The bias lines contribute to increased backside radiation for the active ring.

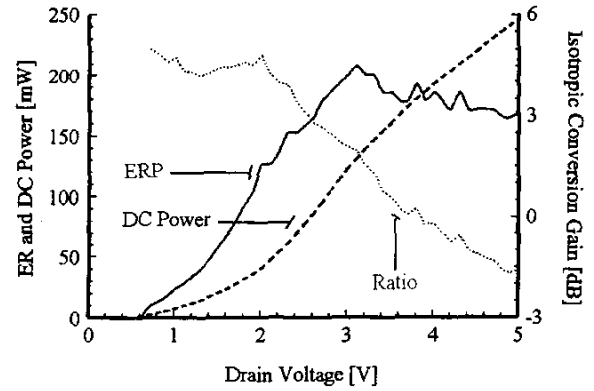

Fig. 6. ERP and DC consumption for $V_{gs} = -1.3\,V$

Since the passive and active antenna patterns closely agree, the passive antenna can be used to calibrate the conversion efficiency of the active antenna. First a known power is transmitted from the passive antenna and the broad-side received power in the far-field is recorded. The received power from the active antenna is then compared to this calibration level. In this way we obtain a maximum dc-rf conversion efficiency of 55%. The isotropic conversion gain is shown in Fig. 6 in dotted line along with the ERP.

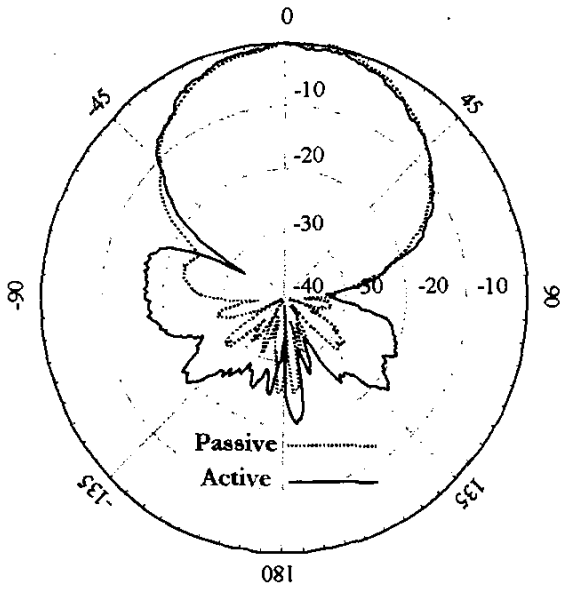

Fig. 7. Active and passive E-plane co-polarized patterns.

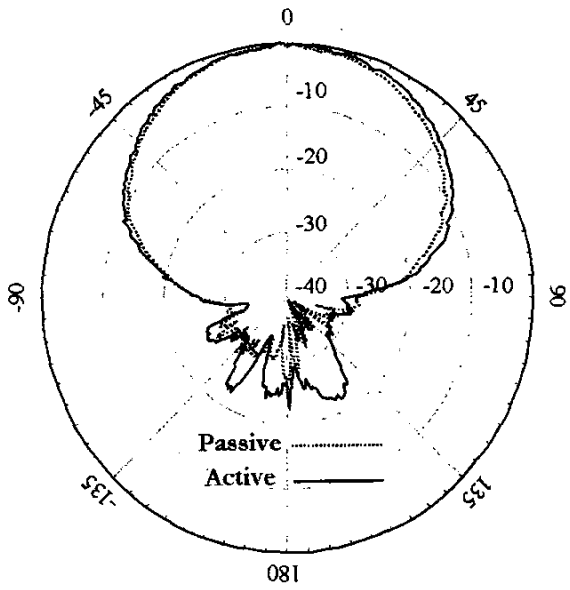

Fig. 8. Active and passive H-plane co-polarized patterns.

VI. Array Design

From Fig. 4 the annular ring radiates as two surface current elements separated by half of a free-space wavelength in the E-plane, enabling a dense array lattice with low mutual coupling between elements. Since the active circuit is internal to the ring, the spacing in the H-plane can also be a half-wavelength. This is made possible by low space-wave coupling in the H-plane [12]. Therefore, an N-element array with a half-wavelength lattice will have an effective area equal to N x effective area of a single element. This will result an array that has the same isotropic conversion as a single element. This is the topic of future work.

VII. Acknowledgment

The authors wish to thank Srdjan Pajić at the University of Colorado for helpful discussions and the Antenna Group at the University of Houston, see Ref. [12]. This work was supported by an ARO MURI in Quasi-Optical Power Combining, grant DAAOH-98-0001. Zoya Popović acknowledges support by a Humboldt Research Award.

References

[1] W.J. Tseng and S.J. Chung, "Analysis and application of a two-port aperture-coupled microstrip antenna," *IEEE Trans. Microwave Theory Tech.*, vol. 46, no. 5, pp. 530–535, May 1998.

[2] R.D. Martinez and R.C. Compton, "High-efficiency FET/microstrip-patch oscillators," *IEEE Antennas and Propagation Magazine*, vol. 36, no. 1, pp. 16–19, Feb. 1994.

[3] K. Chang, K.A. Hummer, and G.K. Gopalakrishnan, "Active radiating element using FET source integrated with microstrip patch antenna," *Electron. Lett.*, vol. 24, no. 21, pp. 1347–1348, Oct. 1988.

[4] D. Bonefacić and J. Bartolić, "Compact active integrated antenna with transistor oscillator and line impedance transformer," *Electron. Lett.*, vol. 36, no. 18, pp. 1519–1521, Aug. 2000.

[5] C. Ho and K. Chang, "New FET active slotline ring antenna," *Electron. Lett.*, vol. 29, pp. 521–522, Mar. 1993.

[6] Z. Popović, R.M. Weikle, M. Kim, and D.B. Rutledge, "A 100-MESFET planar grid oscillator," *IEEE Trans. Microwave Theory Tech.*, vol. 39, pp. 193–200, Feb. 1991.

[7] T.B. Mader and Z. Popović, "The transmission-line high efficiency class-e amplifier," *IEEE Microwave and Guided Wave Lett.*, vol. 5, no. 9, pp. 290–292, Sept. 1995.

[8] S. Pajić and Z. Popović, "A 10-GHz high efficiency active antenna sub-array," *Submitted to the 2002 IEEE-IMS, private communication.*

[9] E.W. Bryerton, W.A. Shiroma, and Z. Popović, "A 5-GHz high efficiency class-e oscillator," *IEEE Microwave and Guided Wave Lett.*, vol. 6, no. 12, pp. 441–443, Dec. 1996.

[10] Y.S. Wu and F.J. Rosenbaum, "Mode chart for microstrip ring resonators," *IEEE Trans. Microwave Theory Tech.*, vol. 21, pp. 487–489, 1973.

[11] A. Bhattacharyya and R. Garg, "Analysis of annular ring microstrip antenna using cavity model," *Archiv für Elektronik und Übertragungstechnik*, vol. 39, pp. 185–189, 1985.

[12] M.A. Khayat, J.T. Williams, D.R. Jackson, and S.A. Long, "Mutual coupling between reduced surface-wave microstrip antennas," *IEEE Trans. Ant. and Prop.*, vol. 48, no. 10, pp. 1581–1593, Oct. 2000.